THE JOURNAL OF BIOLOGICAL CHEMISTRY
Vol. 276, No. 35, Issue of August 31, pp. 32917–32924, 2001

Printed in U.S.A.

Biochemical and Biophysical Evidence for γ_2 Subunit Association with Neuronal Voltage-activated Ca^{2+} Channels*

Received for publication, January 29, 2001, and in revised form, July 3, 2001
Published, JBC Papers in Press, July 5, 2001, DOI 10.1074/jbc.M100787200

Myoung-Goo Kang‡, Chien-Chang Chen‡, Ricardo Felix‡§, Verity A. Letts¶, Wayne N. Frankel¶, Yasuo Mori‖, and Kevin P. Campbell‡

From the ‡Howard Hughes Medical Institute, Department of Physiology and Biophysics, Department of Neurology, University of Iowa College of Medicine, Iowa City, Iowa 52242, ¶The Jackson Laboratory, Bar Harbor, Maine 04609, and the ‖Department of Information Physiology, National Institute for Physiological Sciences, Okazaki 444-8585, Japan

A novel gene (*Cacng2*; γ_2) encoding a protein similar to the voltage-activated Ca^{2+} channel γ_1 subunit was identified as the defective gene in the epileptic and ataxic mouse, stargazer. In this study, we analyzed the association of this novel neuronal γ_2 subunit with Ca^{2+} channels of rabbit brain, and the function of the γ_2 subunit in recombinant neuronal Ca^{2+} channels expressed in *Xenopus* oocytes. Our results showed that the γ_2 subunit and a closely related protein (called γ_3) co-sedimented and co-immunoprecipitated with neuronal Ca^{2+} channel subunits *in vivo*. Electrophysiological analyses showed that γ_2 co-expression caused a significant decrease in the current amplitude of both α_{1B}($\alpha_1$2.2)-class (36.8%) and α_{1A}($\alpha_1$2.1)-class (39.7%) Ca^{2+} channels ($\alpha_1\beta_3\alpha_2\delta$). Interestingly, the inhibitory effects of the γ_2 subunit on current amplitude were dependent on the co-expression of the $\alpha_2\delta$ subunit. In addition, co-expression of γ_2 or γ_1 also significantly decelerates the activation kinetics of α_{1B}-class Ca^{2+} channels. Taken together, these results suggest that the γ_2 subunit is an important constituent of the neuronal Ca^{2+} channel complex and that it down-regulates neuronal Ca^{2+} channel activity. Furthermore, the γ_2 subunit likely contributes to the fine-tuning of neuronal Ca^{2+} channels by counterbalancing the effects of the $\alpha_2\delta$ subunit.

Voltage-activated Ca^{2+} channels play a major role in many fundamental physiological processes including neurotransmission, muscle contraction, intracellular signaling, hormone secretion, and development. Understanding the molecular regulation of these channels is critical for the comprehension of these major physiological phenomena. The high voltage-activated Ca^{2+} channel (called Ca^{2+} channel hereafter) consists of at least three subunits: a main subunit, α_1, and two auxiliary subunits, β and $\alpha_2\delta$ (1, 2). An additional auxiliary subunit, γ, initially detected only in skeletal muscle, has been recently suggested to be a component of the neuronal Ca^{2+} channel complex (3).

The regulation of Ca^{2+} channels by the β and $\alpha_2\delta$ subunits has been extensively studied. Both β and $\alpha_2\delta$ subunits have been found to increase specific ligand binding and to modulate electrophysiological properties of Ca^{2+} channels including current density, voltage dependence, and current kinetics (2). However, much less is known about the function of the skeletal muscle γ subunit (γ_1). Some controversial results of γ_1 effects on current amplitude, voltage dependence, current kinetics, or toxin binding have been observed (4–9).

A molecular genetic study of the stargazer mouse revealed a novel gene responsible for absence epilepsy and ataxia in this animal model. The study suggested that this novel gene encodes a γ subunit for neuronal Ca^{2+} channels that has been named γ_2 (or stargazin). The first 200 amino acids of the γ_2 and γ_1 sequence share 25% identity and 39% similarity. The exon-intron organization and predicted secondary structure of the γ_2 subunit are very similar to that of the γ_1 subunit (3). Previous biophysical studies using recombinant Ca^{2+} channels have indicated an inhibitory role for the γ_2 subunit based on changes in the voltage dependence of steady-state inactivation of the channels (3, 10). In addition, a recent finding of novel γ isoforms (γ_3, γ_4, γ_5) suggests a possibility that a γ gene family originated through tandem and chromosome duplication (11). On the other hand, a recent study has suggested a role of the γ_2 subunit on the trafficking/clustering of AMPA[1] receptors (12).

Mutations in the Ca^{2+} channel subunits have been implicated in the etiology of absence epilepsy and ataxia in mice: four α_{1A} mutations in the tottering, leaner, rolling, and rocker mice (13–15); a β_4 mutation in the lethargic mouse (16); a $\alpha_2\delta$-2 mutation in the ducky mouse (17); and a γ_2 mutation in the stargazer mouse (3). Understanding Ca^{2+} channel regulation at the molecular level will lead to further comprehension of the mechanisms underlying these neurological disorders.

In this study, by showing the association of the γ_2 subunit with other Ca^{2+} channel subunits, we provide biochemical data supporting the hypothesis that the γ_2 subunit is a component of the neuronal Ca^{2+} channel complex. Furthermore, by examining the function of the γ_2 subunit using recombinant α_{1B}- and α_{1A}-class Ca^{2+} channels expressed in *Xenopus* oocytes, we show that the novel γ_2 subunit participates in the modulation of the neuronal Ca^{2+} channels. Our results demonstrate that the γ_2 subunit is a part of the neuronal Ca^{2+} channel complex and has a $\alpha_2\delta$-dependent inhibitory effect on the channel activity.

EXPERIMENTAL PROCEDURES

Partial Purification of Neuronal Ca^{2+} Channels—Brain microsomes were prepared from rabbit and mouse as described previously (18). From the microsomes (200 mg of rabbit and 50 mg of mouse micro-

* The costs of publication of this article were defrayed in part by the payment of page charges. This article must therefore be hereby marked "*advertisement*" in accordance with 18 U.S.C. Section 1734 solely to indicate this fact.

§ Present address: Dept. of Physiology, Biophysics and Neuroscience, Cinvestav-National Polytechnic Institute, Mexico 07300.

** Investigator of the Howard Hughes Medical Institute. To whom correspondence should be addressed: Howard Hughes Medical Inst., University of Iowa College of Medicine, 400 EMRB, Iowa City, IA 52242-1101. Tel.: 319-335-7867; Fax: 319-335-6957; E-mail: kevin-campbell@uiowa.edu.

[1] The abbreviations used are: AMPA, α-amino-3-hydroxyl-5-methyl-4-isoxazole propionic acid; WGA, wheat germ agglutinin; MES, 4-morpholineethanesulfonic acid.

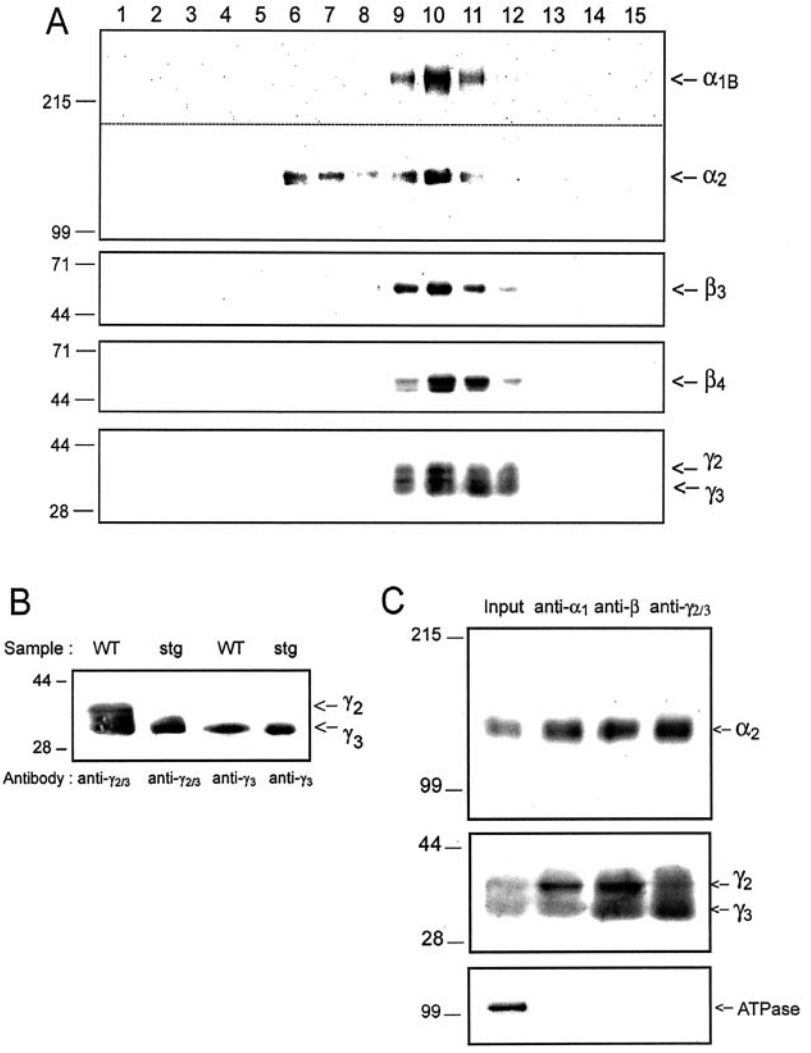

FIG. 1. **Association of the γ_2 and γ_3 subunits with other neuronal Ca^{2+} channel subunits.** *A*, sucrose gradient fractionation of neuronal Ca^{2+} channels. The *numbers* at the *top* indicate the fraction of the sucrose gradient from top to bottom. Equal volume of proteins (80 μl) were loaded in each *lane*. *B*, characterization of the protein bands recognized by the $\gamma_{2/3}$ or γ_3 antibodies. The protein samples (100 μg each) were from the stargazer mice (*stg*) or their wild-type littermates (*WT*). The antibodies used for the Western blot analyses are indicated at the *bottom*. *C*, co-immunoprecipitation of the γ_2 and γ_3 subunits by antibodies specific for neuronal Ca^{2+} channel subunits. The first lane (*Input*) was loaded with the protein aliquot saved before immunoprecipitation. Sheep 37 (anti-α_1), $VD2_1$ (anti-β), and Rabbit 239 (anti-$\gamma_{2/3}$), specific for the Ca^{2+} channel subunits, $\alpha_{1A/B}$, β, and $\gamma_{2/3}$, respectively, were used for immunoprecipitation. Equal amounts of proteins (50 μg) were loaded in each lane. The antibodies used for immunoprecipitation are indicated at the *top* of the other lanes. Molecular mass standards ($\times 10^{-3}$) are indicated on the *left*. Data are representative of at least three independent experiments.

somes), the Ca^{2+} channel complexes were extracted with solubilization buffer containing (in mM) 50 Tris-HCl, pH 7.4, 500 NaCl, a mixture of protease inhibitors, and 1% digitonin (Biochemica & Synthetica, Staad, Switzerland) by rotating end-over-end at 4 °C for 1 h. After centrifugation at 142,413 × *g* for 37 min, solubilized proteins in the supernatant were then mixed with wheat germ agglutinin (WGA)-agarose beads (Vector Laboratories, Burlingame, CA) and rotated end-over-end at 4 °C overnight. After washing three times with three bed volumes of ice-cold wash buffer (Buffer I containing (in mM) 50 Tris-HCl, pH7.4, 500 NaCl, a mixture of protease inhibitors, and 0.1% digitonin), WGA-bound proteins were eluted with elution buffer (Buffer I + 0.3 M *N*-acetyl-D-glucosamine (Sigma)). The WGA eluant was concentrated to 0.5 ml in an Ultrafree-15 centrifugal filter device (Millipore, Bedford, MA), and applied to a 5–30% sucrose density gradient (Buffer I + 5–30% sucrose). The gradients were centrifuged at 215,000 × *g* for 90 min. Fractions (0.8 ml) were collected from the top of the gradients using a density gradient fractionator (Auto Densi-flow, Labconco, Kansas City, MO).

Antibodies—Polyclonal antibodies, Sheep 37, Sheep 46, Rabbit 136, Sheep 49, Rabbit 145, and Rabbit 239, specific for the Ca^{2+} channel subunits, $\alpha_{1A/B}$, α_{1B}, α_2, β_3, β_4, and $\gamma_{2/3}$, respectively, have been described previously (3, 19–22). The γ_3 subunit-specific polyclonal antibody, Rabbit 302, was generated by Genemed Synthesis (South San Francisco, CA) against an amino-terminal cysteine 12-mer peptide (Research Genetics, Huntsville, AL) corresponding to residues 273–281 of mouse γ_3 subunit primary structure. Monoclonal antibody $VD2_1$, which recognizes all Ca^{2+} channel β subunits, has been described previously (23).

Immunoprecipitation of Ca^{2+} Channel Subunits—Antibodies were cross-linked to protein A-agarose beads (Santa Cruz Biotechnology, Santa Cruz, CA) using dimethyl pimelimidate as described elsewhere (24). The partially purified neuronal Ca^{2+} channel complexes were incubated with the antibody-protein A-agarose beads at 4 °C overnight on a rolling platform. After washing the beads three times with three bed volumes of ice-cold wash buffer (Buffer I), Ca^{2+} channel subunits bound to the antibodies were eluted with 50 mM glycine-HCl, pH 2.5, and the pH was immediately neutralized with 0.1 volume of 1 M Tris-HCl, pH 8.0.

Western Blot Analysis—The WGA eluants, sucrose gradient fractions, or immunoprecipitated proteins were resolved in 4–15% gradient SDS-polyacrylamide gel electrophoresis under reducing condition (2% β-mercaptoethanol) and transferred to polyvinylidene difluoride membrane (Millipore). The polyvinylidene difluoride blots were cut and probed separately with affinity-purified antibodies against the subunits of the Ca^{2+} channel complex or Na^+/K^+ ATPase at 4 °C overnight. After staining with Horseradish peroxidase-conjugated secondary antibodies (Roche Molecular Biochemicals), the blots were developed by enhanced chemiluminescence (ECL) (SuperSignal™ or DuraSignal™, Pierce, Rockford, IL), and imaged using an image capturing system (MultiImage™, Alpha Innotech, San Leandro, CA).

cDNA Clones—cDNA clones used were as follows: rabbit brain α_{1A} cDNA (4), rat brain $\alpha_{1B\text{-}b}$ cDNA (25), rat brain β_3 (GenBank™ accession no. M88751), rat brain $\alpha_2\delta_b$ (GenBank™ accession no. M86621), rabbit skeletal γ_1 (26), and mouse brain γ_2 (3). As expression vectors, pcDNA3 (Invitrogen, Carlsbad, CA) was used for $\alpha_2\delta_b$, γ_1, and γ_2; pSP72 (Promega, Madison, WI) for α_{1A}; pBSTA (27) for α_{1B}; and pGEM3 (Promega) for β_3.

Preparation of Xenopus Oocytes—Female *Xenopus laevis* were purchased from Nasco (Fort Atkinson, WI). Frogs were maintained under a 12-h light/12-h dark cycle at 18 °C. Ovarian lobes were surgically removed from frogs that had been anesthetized by hypothermia. To facilitate injection and recording, the follicle cell layer was enzymatically digested with 2 mg/ml collagenase type I (Sigma) for 70 min in Ca^{2+}-free OR-2 solution containing (in mM) 82.5 NaCl, 2.5 KCl, 1 $MgCl_2$, and 5 HEPES-NaOH, pH 7.6. Oocytes at stages V and VI were selected and washed several times with Ca^{2+}-free OR-2 solution and subsequently

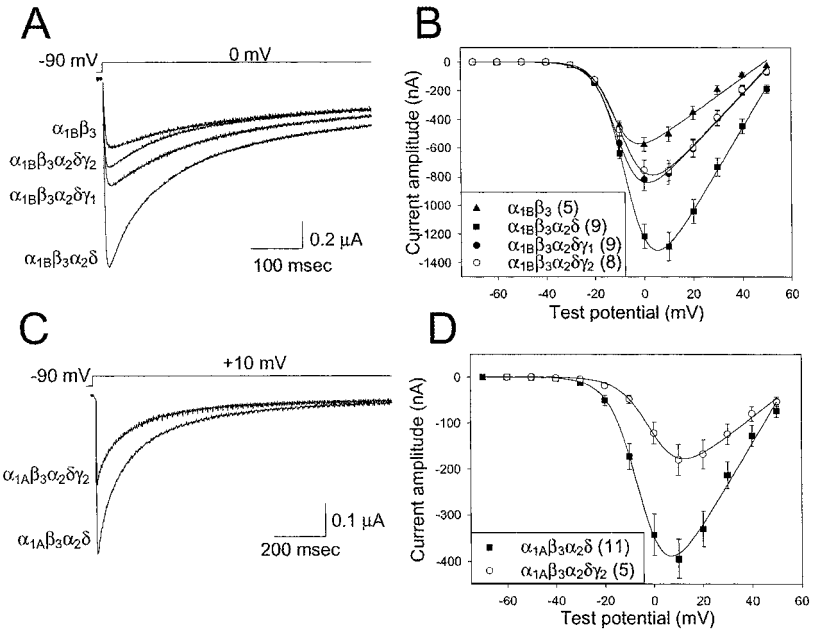

FIG. 2. **Regulation of current amplitude of neuronal Ca^{2+} channels by the γ_2 subunit.** *A*, superimposed current traces of α_{1B}-class channels. *B*, current-voltage (*I-V*) relationships of α_{1B}-class channels. *C*, superimposed current traces of α_{1A}-class channels. *D*, *I-V* relationships of α_{1A}-class channels. Current traces were averaged from three representative cells in each group of oocytes, and the voltage protocol is shown *above* the *traces* (*A* and *C*). Ca^{2+} channel subunit composition is listed in the *inset*, and the number of recorded cells is indicated in parentheses (*B* and *D*). Data are representative of at least three independent experiments.

placed in ND96 solution containing (in mM) 96 NaCl, 15 KCl, 1 $MgCl_2$, 1.8 $CaCl_2$, 2.5 sodium pyruvate, and 5 HEPES-NaOH, pH 7.6, plus 1% penicillin/streptomycin. Before cRNA injection, the oocytes were incubated overnight at 18 °C in ND96 solution.

Heterologous Expression of Ca^{2+} Channel Subunits—Linearized plasmids were *in vitro* transcribed with T7 (or SP6 for α_{1A}) polymerase transcription kits (mMESSAGE mMACHINE, Ambion, Austin, TX). Transcribed cRNA was purified using the RNeasy kit (Qiagen, Stanford, CA), and then analyzed by gel electrophoresis and stored at −20 °C. Oocytes were injected with 46 nl of various cRNA mixtures of Ca^{2+} channel subunits using a nano-injector (Drummond, Broomall, PA) at the following ratio 2:2:1:1 = α_1:$\alpha_2\delta$:β_3:γ. The amount of cRNA injected was varied in each experiment to get current amplitudes under optimal voltage control. Injected oocytes were incubated at 18 °C in ND96 solution for 4–5 days before electrophysiological recording.

Electrophysiological Recordings and Data Analyses—Ba^{2+} currents through Ca^{2+} channels were recorded by the two-electrode voltage-clamp technique (28) with a TEV-200 amplifier (Dagan, Minneapolis, MN) at room temperature. Microelectrodes were pulled from borosilicate glass capillary (Kimble Glass Co., Vienland, NJ) using a horizontal puller (Sutter Instrument, Novato, CA). Both voltage and current electrodes were filled with 3 M KCl and had initial tip resistances of 0.5–1.0 megaohm. The recording chamber (500-μl volume) was filled with recording solution containing (in mM) 10 $Ba^{2+}(OH)_2$, 2 KCl, 0.1 EGTA, 80 NaOH, 1 niflumic acid, and 10 HEPES-MES, pH 7.2. Ca^{2+}-activated Cl^- outward currents were minimized by the use of Ba^{2+} as charge carrier, low concentration of Cl^- in the solutions, and niflumic acid (a Cl^- current blocker). Unless otherwise indicated, test potentials were applied for 2 s from a holding potential of −90 mV using pClamp 6 software (Axon Instruments, Foster City, CA). Output signals were filtered at 1 kHz and sampled at 5 kHz. Data were digitized with a TL-1 interface (Axon Instruments), and the results were analyzed by pClamp 6 and SigmaPlot 4.01 (SPSS Inc., Chicago, IL). Leak and capacitance currents were subtracted on-line by a P/6 protocol. If present, residual capacitance was blanked.

I-V curves were fitted using a modified Boltzmann equation of the form: $I = [G_{max}(V_m - E)]/[1 + \exp(-(V_m - V_{½})/k)]$, where I represents current amplitude, G_{max} maximum conductance, V_m test potential, E reversal potential, $V_{½}$ potential of half-activation, and k slope factor. Steady-state activation curves were also described by a modified Boltzmann equation: $G = G_{max}/[1 + \exp((V_m - V_{½})/k)]$, where G represents conductance obtained from the equation: $G = I/(V_m - E)$. Steady-state inactivation curves were also described by a modified Boltzmann equation: $I = I_{max}/[1 + \exp((V_m - V_{½})/k)]$. To obtain the estimates of the activation and inactivation rates, data were fit to single- and two-exponential equations, respectively, using the fitting routines of pClamp 6 software.

Statistical Analysis—Each experiment was repeated at least three times using different batches of oocytes or brain from different animals. Data are presented as means ± S.E. of the mean, and the number of oocytes is indicated in the figures and Table I. Data were analyzed by two-way analysis of variance. When significant *F*-values were encountered, the different treatments were compared using the Tukey multiple comparisons test. Probability (p) of 0.05 or less was considered

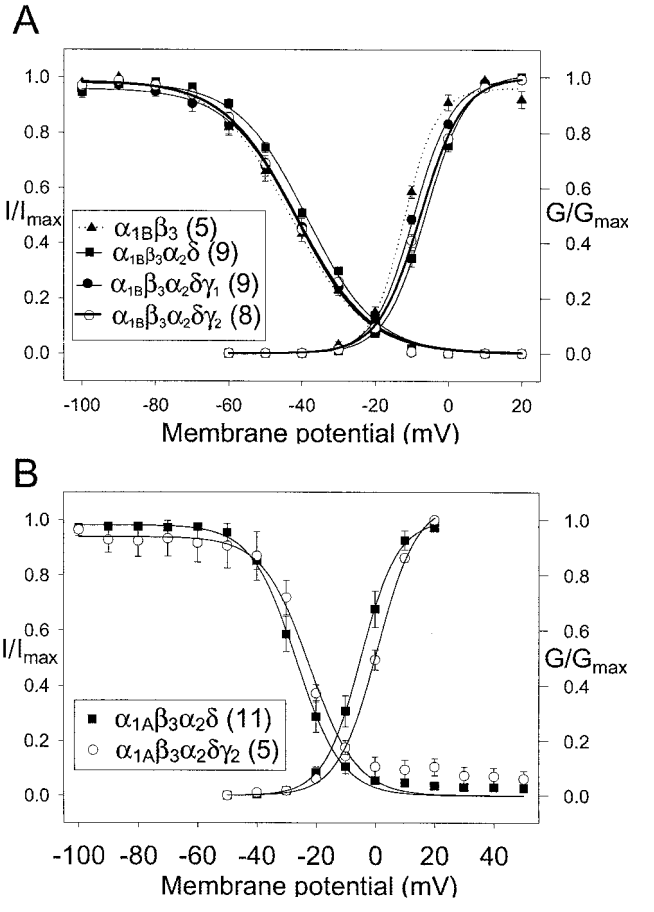

FIG. 3. **Modulation of voltage dependence of neuronal Ca^{2+} channels by the γ_2 subunit.** *A & B*, Superimposed plots of steady-state activation (G/G_{max}) and inactivation (I/I_{max}) curves from α_{1B}-class (*A*) and α_{1A}-class (*B*) channels. Ca^{2+} channel subunit composition is listed in the *inset*, and the number of recorded cells is indicated in *parentheses*. Data are representative of at least three independent experiments.

TABLE I

Kinetic parameters of the α_{1B}- and α_{1A}-class Ca^{2+} channels

Values are presented as mean ± S.E. *, $p < 0.05$, **, $p < 0.001$ (respect to $\alpha_1\beta_3\alpha_2\delta$); V, membrane potential, $V_{1/2}$, membrane potential for half-maximal activation (or inactivation); k, slope factor; τ_{act}, time constant of activation; n, cell number.

Properties	$\alpha_{1B}\beta_3$	$\alpha_{1B}\beta_3\alpha_2\delta$	$\alpha_{1B}\beta_3\alpha_2\delta\gamma_1$	$\alpha_{1B}\beta_3\alpha_2\delta\gamma_2$	$\alpha_{1A}\beta_3\alpha_2\delta$	$\alpha_{1A}\beta_3\alpha_2\delta\gamma_2$
Steady-state activation parameters						
$V_{1/2}$ (mV)	−12.10 ± 0.69**	−5.63 ± 0.87	−9.42 ± 0.36**	−7.54 ± 0.59	−4.35 ± 2.03	−0.61 ± 0.77
k (mV)	−4.61 ± 0.13*	−5.59 ± 0.29	−5.36 ± 0.12	−5.68 ± 0.18	−5.42 ± 0.19	−6.54 ± 0.44**
n	5	9	9	8	11	5
Steady-state inactivation parameters						
$V_{1/2}$ (mV)	−43.34 ± 1.26	−38.86 ± 0.81	−42.44 ± 1.73	−41.95 ± 0.89	−26.52 ± 6.51	−23.65 ± 2.88
k (mV)	10.13 ± 0.55	9.51 ± 0.33	9.92 ± 0.76	10.22 ± 0.36	6.51 ± 0.34	10.39 ± 2.09*
n	6	10	9	9	11	5

Properties	$\alpha_{1B}\beta_3$	$\alpha_{1B}\beta_3\alpha_2\delta$	$\alpha_{1B}\beta_3\alpha_2\delta\gamma_1$	$\alpha_{1B}\beta_3\alpha_2\delta\gamma_2$
Time constants of activation (ms)				
τ_{act} at −20 mV	3.87 ± 0.05**	2.31 ± 0.09	3.99 ± 0.24**	3.12 ± 0.22*
τ_{act} at −10 mV	4.28 ± 0.15**	2.43 ± 0.07	4.08 ± 0.26**	2.98 ± 0.11*
τ_{act} at 0 mV	2.70 ± 0.16*	1.88 ± 0.12	2.40 ± 0.13*	2.04 ± 0.11
n	5	9	9	8

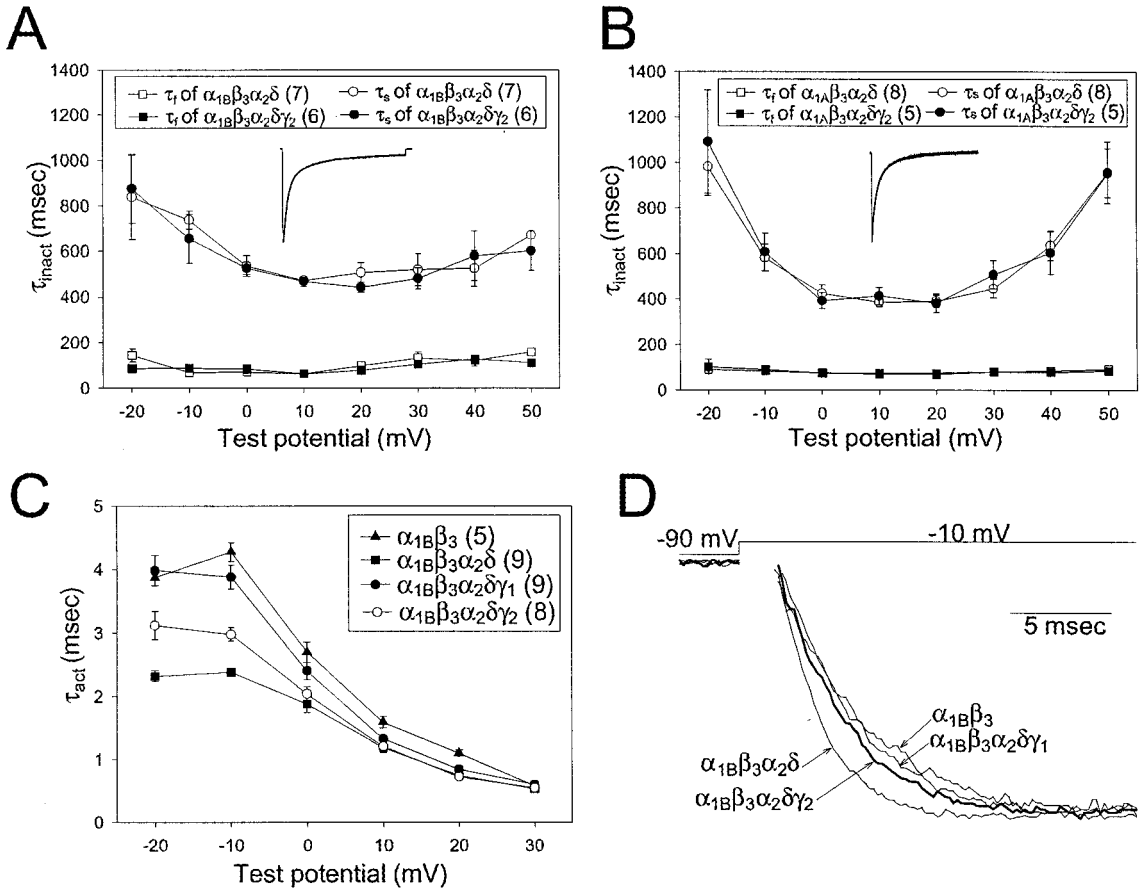

FIG. 4. **Modulation of current kinetics of neuronal Ca^{2+} channels by the γ_2 subunit.** *A* and *B*, superimposed plotting of α_{1B}-class (*A*) and α_{1A}-class (*B*) channel inactivation time constants (τ_{inact}) as a function of the voltage step. *Squares* and *circles* present fast (τ_f) and slow (τ_s) inactivation time constants, respectively. Examples of a current trace of $\alpha_1\beta_3\alpha_2\delta\gamma_2$ at 10 mV and two-exponential fit (*thick line*) to the inactivating current are shown in the *inset*. *C*, superimposed plots of α_{1B}-class channel activation time constants (τ_{act}) as a function of the voltage step. Ca^{2+} channel subunit composition is listed in the *inset*, and the number of recorded cells is indicated in *parentheses* (*A–C*). *D*, superimposed current traces showing the time course of α_{1B}-class channel activation. Current traces were averaged from three representative cells in each group of oocytes (*A*, *B*, and *D*). Data are representative of at least three independent experiments.

significant. The statistical analysis was performed using SYSTAT 7.0 (SPSS Inc.).

RESULTS

Association of the γ_2 Subunit with Neuronal Ca^{2+} Channel Subunits—The association of the γ_2 subunit with the neuronal Ca^{2+} channel complex was investigated through sucrose gradient fractionation analysis as follows. Ca^{2+} channel complexes were partially purified from the rabbit cerebellum as described under "Experimental Procedures." Western blot analysis of sucrose gradient fractions with anti-α_{1B}, anti-α_2, anti-β_3, anti-β_4, and anti-$\gamma_{2/3}$ antibodies showed that the α_{1B}, α_2, β_3, β_4, and $\gamma_{2/3}$ co-sedimented in fractions 9–12 (Fig. 1*A*). Considering the much smaller molecular masses of the $\gamma_{2/3}$ (34 and 38-kDa), β_3 (57-kDa) or β_4 (57-kDa) subunits compared with that of the α_{1B}

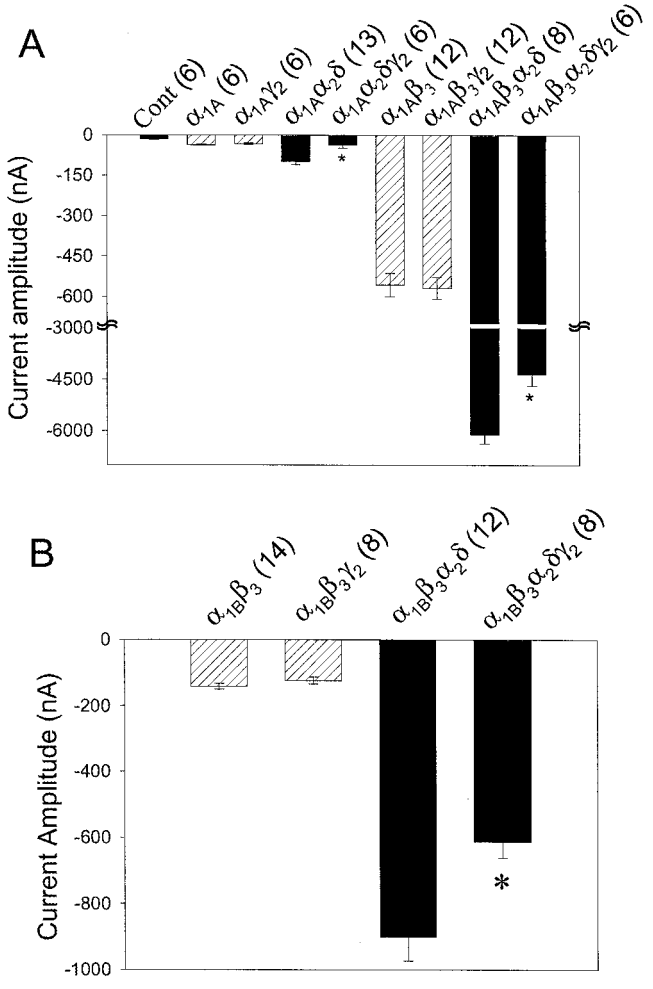

FIG. 5. **Regulation of current amplitude of neuronal Ca^{2+} channels by the γ_2 subunit in various subunit composition.** *A* and *B*, comparison of peak current amplitude of α_{1A}- and α_{1B}-class channels in various combinations of subunits as listed. *Asterisks* (*) at $\alpha_{1A}\alpha_2\delta\gamma_2$, $\alpha_{1A}\beta_3\alpha_2\delta\gamma_2$, or $\alpha_{1B}\beta_3\alpha_2\delta\gamma_2$ denote significant differences ($p < 0.02$) in current amplitude compared with $\alpha_{1A}\alpha_2\delta$, $\alpha_{1A}\beta_3\alpha_2\delta$, or $\alpha_{1B}\beta_3\alpha_2\delta$, respectively. The number of recorded cells is indicated in *parentheses* within the legends representing subunit composition. Data are representative of at least three independent experiments.

subunit (230-kDa), co-sedimentation of the α_{1B}, β_3, β_4, and $\gamma_{2/3}$ subunits suggests that the $\gamma_{2/3}$ subunits are in a complex with the α_{1B}, β_3, and β_4 subunits. In addition, the co-sedimentation of the α_{1A} subunit with γ_2 subunits was tested by probing the sucrose gradient blot with Sheep 37 antibody (anti-$\alpha_{1A/\beta}$) and an anti-α_{1A} antibody from Alomone Laboratories (Jerusalem, Israel). The α_{1A} and $\gamma_{2/3}$ subunits were detected in the same fractions of the sucrose gradient (data not shown).

Since the anti-$\gamma_{2/3}$ antibody recognized two or three bands (Fig. 1*A*), the WGA eluants from the whole brain of the stargazer mice or their wild-type littermates were analyzed through Western blot analysis with two different antibodies against the γ_2 or γ_3 subunits (Fig. 1*B*). The anti-$\gamma_{2/3}$ antibody was raised against a peptide corresponding to the carboxyl-terminal residues 312–323 of the γ_2 sequence (3), which is very similar to the carboxyl-terminal residues 304–315 of the γ_3 sequence (10). The upper band (38 kDa) was not detected in the blot of the stargazer mice (Fig. 1*B*, *second lane*) by the anti-$\gamma_{2/3}$ antibody. Furthermore, the anti-γ_3 antibody, raised against the peptide representing the residues 273–281 unique to the γ_3 sequence, recognized only the 34-kDa band in both wild-type and stargazer mouse blots (Fig. 1*B*, *third* and *fourth lanes*, respectively). Therefore, we could conclude that the 38-kDa band represents the γ_2 subunit and the 34-kDa band represents the γ_3 subunit. The identity of the middle band (about 36 kDa) recognized by anti-$\gamma_{2/3}$ antibody is still under investigation.

To confirm that the co-sedimentation of the γ_2 and γ_3 subunits with the α_{1B} subunits was due to a specific interactions with the Ca^{2+} channel complex, sucrose gradient fractions (fraction 9–12) containing both $\alpha_{1A/B}$ and γ_2 subunits (Fig. 1*A*) were pooled and subjected to immunoprecipitation analyses as described under "Experimental Procedures." Polyclonal anti-α_1 antibody recognizing $\alpha_{1A/B}$ subunits of Ca^{2+} channel immunoprecipitated both the γ_2 and γ_3 subunits (Fig. 1*C*, *second lane*). Monoclonal anti-β antibody, which recognizes all Ca^{2+} channel β subunits, was also able to immunoprecipitate the γ_2 and γ_3 subunits (Fig. 1*C*, *third lane*). The same blots were probed with the anti-α_2 antibodies to show that the whole neuronal Ca^{2+} channel complexes were immunoprecipitated. Furthermore, the α_2 band (140 kDa) was detected by immunoprecipitation with the anti-$\gamma_{2/3}$ antibody (Fig. 1*C*, *fourth lane*). In addition, to rule out the possibility of nonspecific precipitation by these antibodies, the same blot was probed with an anti-Na^+/K^+ ATPase antibody (Affinity Bioreagents, Inc., Golden, CO). The Na^+/K^+ ATPase was detected in the pooled fraction of sucrose gradient before immunoprecipitation (Fig. 1*C*, *first lane*, *Input*), but was not immunoprecipitated with any of the calcium channel subunit antibodies (Fig. 1*C*, *second* through *fourth lanes*). These immunoprecipitation results strongly suggest that the γ_2 and γ_3 subunits bind to neuronal Ca^{2+} channel complexes composed of $\alpha_{1A/B}$, $\alpha_2\delta$, and β subunits.

Taken together, the co-sedimentation and co-immunoprecipitation of the γ_2 and γ_3 subunits with other neuronal Ca^{2+} channel subunits constitute what is to our knowledge the first biochemical evidence that the γ_2 and γ_3 subunits are structural components of neuronal Ca^{2+} channel complexes of the α_{1B}- and α_{1A}-class.

Effect of the γ_2 Subunit on the Current Amplitude of Recombinant α_{1B}- and α_{1A}-class Ca^{2+} Channels—Having shown that the γ_2 subunit is an important part of the neuronal Ca^{2+} channels, we next explored the effects of this subunit on Ba^{2+} current through $\alpha_1\beta_3\alpha_2\delta$ channels using *Xenopus* oocytes as an expression system. Fig. 2*A* shows representative current traces from four groups of oocytes injected with different subunit compositions. Co-expression of γ_2 or γ_1 significantly decreased current amplitude. This effect was consistently observed at most potentials examined, as shown in Fig. 2*B*. In the representative experiments shown in Fig. 2 (*A* and *B*), peak current amplitude was -1.22 ± 0.08 μA ($n = 9$) in cells expressing $\alpha_{1B}\beta_3\alpha_2\delta$ and significantly decreased to -0.76 ± 0.07 μA ($n = 8$) and -0.82 ± 0.08 μA ($n = 9$) upon co-expression of γ_2 ($p < 0.001$) and γ_1 ($p < 0.003$), respectively. Overall, the cells co-expressing γ_2 ($n = 31$) showed 36.8 ± 1.6% decrease of peak current amplitude compared with the cells expressing only $\alpha_{1B}\beta_3\alpha_2\delta$ ($n = 25$). A similar effect of the γ_2 subunit on current amplitude was observed in oocytes expressing α_{1A}-class Ca^{2+} channels (Fig. 2, *C* and *D*). Fig. 2*C* shows the current traces from two groups of oocytes in the absence and presence of γ_2. In this case, peak amplitude decreased significantly from -0.40 ± 0.04 μA ($n = 11$) to -0.18 ± 0.03 μA ($n = 5$) in cells expressing $\alpha_{1A}\beta_3\alpha_2\delta$ and $\alpha_{1A}\beta_3\alpha_2\delta\gamma_2$ ($p < 0.007$), respectively. This effect was consistently observed in the ±40 mV range (Fig. 2*D*). Overall, the cells co-expressing γ_2 ($n = 36$) showed 39.7 ± 5.9% decrease of peak current amplitude compared with the cells expressing only $\alpha_{1A}\beta_3\alpha_2\delta$ ($n = 25$).

Effect of the γ_2 Subunit on Voltage Dependence of α_{1B}- and α_{1A}-class Ca^{2+} Channels—Since it could be possible that the effect of the γ subunits on current amplitude is due to a change

in the voltage dependence of steady-state activation and/or inactivation, we next studied the voltage-dependent properties of activation and inactivation of α_{1B}- and α_{1A}-class Ca^{2+} channels. Fig. 3 (*A* and *B*) shows the steady-state activation of the recombinant Ca^{2+} channels plotted as a function of the test potential. Data were fitted with a modified Boltzmann equation to calculate potentials for half-maximal activation and slope factors, and the results are summarized in Table I. Although there was no significant shift of the membrane potential for half-maximal activation in both classes of channels by γ_2 co-expression, the slope factor of the activation curve for $\alpha_{1A}\beta_3\alpha_2\delta$ channel was affected by γ_2 co-expression. In addition, the properties of voltage-dependent inactivation were studied by applying 2.0-s pre-pulses ranging successively from −100 to 50 mV in 10-mV voltage steps, followed by a 0.5-s step depolarization to 0 mV. The averaged data were plotted as a function of voltage and fitted with a modified Boltzmann equation as shown in Fig. 3 (*A* and *B*), and potentials for half-maximal inactivation and slope factors are summarized in Table I. Although γ_2 co-expression did not affect significantly the membrane potential for half-maximal inactivation of the $\alpha_1\beta_3\alpha_2\delta$ channel, the slope factor of the steady state inactivation curve for $\alpha_{1A}\beta_3\alpha_2\delta$ channel was affected by the co-expression of the γ_2 subunit (Table I).

Effect of the γ_2 Subunit on Kinetics of α_{1B}- and α_{1A}-class Ca^{2+} Channels—The inactivation kinetics of the α_{1B}- and α_{1A}-class channels was assayed by applying a 2.0-s pulse from a −90 mV holding potential to various membrane potentials. Inactivation time constants were then obtained by fitting the decaying phase of the currents to a two-exponential equation. In Fig. 4 (*A* and *B*), these time constants are plotted as function of the test potential. The properties of inactivation kinetics were similar in both α_{1B}- and α_{1A}-class channels in terms of inactivation rate and the voltage dependence of inactivation rate. Fast inactivation time constants (τ_f) in both types of channels were around 100 ms in a wide range of test potentials. In contrast, the voltage dependence of slow inactivation in both α_{1B}- and α_{1A}-class channels showed a U-shape. Similar U-shaped voltage dependence of inactivation rate of α_{1B}-class channels was reported previously (29). Slow inactivation time constants (τ_s) were highest at −20 mV and decreased to about 400 ms around 10 mV, and then increased again at voltages above 30 mV. Overall, inactivation kinetics of neither α_{1B}- nor α_{1A}-class Ca^{2+} channels was modified by γ_2 co-expression (Fig. 4, *A* and *B*). For example, at 10 mV (peak current potential), τ_f values were 61.80 ± 1.85 ms ($n = 7$) and 62.33 ± 2.33 ms ($n = 6$), and τ_s 473.20 ± 19.09 ms ($n = 7$) and 469.00 ± 21.31 ms ($n = 6$) in $\alpha_{1B}\beta_3\alpha_2\delta$ and $\alpha_{1B}\beta_3\alpha_2\delta\gamma_2$ channels, respectively (Table I).

Similarly, the effects of the γ_2 subunit on activation kinetics were analyzed by comparing the activation time constant (τ_{act}) in a series of test potentials (Fig. 4*C*) ranging from −20 to +30 mV. Time constants were measured by fitting the rising phase of current to a single-exponential equation. As illustrated in Fig. 4*C*, the activation of currents was significantly decelerated by γ_2 co-expression at negative potentials (see also Table I). The differences in activation at a test potential of −10 mV are depicted in Fig. 4*D* using representative normalized current traces from a group of oocytes expressing α_{1B}-class channels in the absence and presence of the γ subunits. These traces clearly illustrate that the rising phase of the currents in the presence of the γ subunits activate slower than the currents recorded in oocytes expressing only $\alpha_{1B}\beta_3\alpha_2\delta$. Consistent with this, at −10 mV τ_{act} values were 2.43 ± 0.07 ms ($n = 9$) and 2.98 ± 0.11 ms ($n = 8$) in $\alpha_{1B}\beta_3\alpha_2\delta$ and $\alpha_{1B}\beta_3\alpha_2\delta\gamma_2$ channels, respectively ($p < 0.014$). The activation kinetics of α_{1A}-class channel was analyzed similarly; however, in this case γ_2 co-expression did not change activation kinetics (data not shown).

The Inhibitory Effect of the γ_2 Subunit Is Dependent on the Co-expression of the $\alpha_2\delta$ Subunit—To investigate the mechanism of the γ_2 inhibitory effect on current amplitude, we analyzed the peak currents through α_{1A}-class Ca^{2+} channel in various combinations of auxiliary subunits in the presence or absence of the γ_2 subunit (Fig. 5*A*). The amount of cRNA injected for the experiment presented in Fig. 5*A* was much higher than that of the other experiments to obtain a better expression of α_{1A} subunits without other auxiliary subunits. The current amplitude of α_{1A} channels was not significantly modified by the γ_2 co-expression; current amplitude of α_{1A} and $\alpha_{1A}\gamma_2$ channels were −37 ± 2.2 nA ($n = 6$) and −33 ± 2.8 nA ($n = 6$), respectively. In contrast, γ_2 co-expression decreased the current amplitude of α_{1A} channels when the $\alpha_2\delta$ subunit was present. The current amplitude decreased from −99 ± 1.1 nA ($n = 13$) in $\alpha_{1A}\alpha_2\delta$ channels to −37 ± 1.1 nA ($n = 6$) in $\alpha_{1A}\alpha_2\delta\gamma_2$ channels ($p < 0.018$). Interestingly, the current amplitude of $\alpha_{1A}\beta_3$ channel was not affected by γ_2 co-expression; the current amplitude of $\alpha_{1A}\beta_3$ and $\alpha_{1A}\beta_3\gamma_2$ channels was −560 ± 42 nA ($n = 6$) and −570 ± 40 nA ($n = 12$), respectively. However, in the $\alpha_{1A}\beta_3\alpha_2\delta$ channels, the current amplitude significantly decreased from −6111 ± 270 nA ($n = 8$) to −4357 ± 328 nA ($n = 6$) by γ_2 co-expression ($p < 0.02$).

Similarly, a current amplitude analysis performed in the α_{1B}-class Ca^{2+} channels also showed a significant inhibitory effect by the γ_2 subunit only when $\alpha_2\delta$ was co-expressed (Fig. 5*B*). The current amplitude of $\alpha_{1B}\beta_3$ channels was not affected by γ_2 co-expression; the current amplitude of $\alpha_{1B}\beta_3$ and $\alpha_{1B}\beta_3\gamma_2$ channels was −141 ± 9.1 nA ($n = 14$) and −123 ± 11 nA ($n = 8$), respectively. On the other hand, in the $\alpha_{1B}\beta_3\alpha_2\delta$ channels, the current amplitude significantly decreased from −900 ± 73 nA ($n = 12$) to −613 ± 48 nA ($n = 8$) by γ_2 co-expression ($p < 0.02$). Therefore, it seems that the inhibitory effect of the γ_2 subunits on neuronal Ca^{2+} channel current amplitude is dependent on the $\alpha_2\delta$ co-expression.

DISCUSSION

Interaction of the γ_2 Subunit with the Neuronal Ca^{2+} Channel Complex—In this study, the association of the γ_2 subunit with neuronal Ca^{2+} channel complexes was analyzed through sucrose density gradient fractionation and immunoprecipitation. Both biochemical analyses consistently demonstrated that the γ_2 subunits are associated with neuronal Ca^{2+} channels (α_{1B}- and α_{1A}-class). In addition, the biochemical analyses in this study also showed, for the first time, that the protein expression of the γ_2 subunit is totally absent in the brain of the stargazer mouse and that the γ_3 subunit is also associated with the neuronal Ca^{2+} channels.

Our biochemical and biophysical data strongly suggest that γ_2 is an auxiliary subunit of neuronal Ca^{2+} channels like the β and $\alpha_2\delta$ subunits. As shown in Fig. 1, the γ_2 association with neuronal Ca^{2+} channels was confirmed by both co-sedimentation and co-immunoprecipitation of the γ_2 subunit with the other components of neuronal Ca^{2+} channels. Additionally, our biophysical studies suggest an inhibitory role for the γ_2 subunit on neuronal Ca^{2+} channel activity. This is consistent with a recent patch clamp study in brain slices of the stargazer mouse that showed the current amplitude of voltage-activated Ca^{2+} channel in thalamocortical relay neurons is significantly increased (30). Taken together, these data strongly suggest that the γ_2 subunit is a component of neuronal Ca^{2+} channels *in vivo*.

Interestingly, another recent study by Chen *et al.* (12) suggested that the γ_2 subunit is involved in the regulation of synaptic targeting/clustering of AMPA receptors. This raises an intriguing possibility that the γ_2 subunit is involved not only in Ca^{2+} current modulation but also in AMPA receptor traf-

ficking. However, Chen *et al.* showed no significant change of the Ca^{2+} channel current in the isolated cerebellar granule cells between the stargazer and wild-type mice. One possible explanation for the unaltered Ca^{2+} channel current could be the compensation for the loss of γ_2 by other γ isoforms. Consistent with this possibility, five γ isoforms have been reported (3, 10, 11, 26, 31). Furthermore, it has been demonstrated that the loss of β_4 subunit did not cause any significant change in the Ca^{2+} channel current of Purkinje neurons from lethargic mouse, due to increased steady-state association of α_1 subunit with the remaining β_{1-3} isoforms (32). Similar functional compensation might occur in the Ca^{2+} channels of the cerebellar granule cells of the stargazer mouse.

In the sucrose gradient analysis, the $\alpha_2\delta$ subunit predominantly sedimented in fractions 9–12, where all other subunits sedimented. However, a peak of $\alpha_2\delta$ was also seen in earlier fractions (Fig. 1*A*). This might represent a pool of $\alpha_2\delta$ that dissociates from the Ca^{2+} channel complex during the purification process.

The Modulation of Neuronal Ca^{2+} Channels by the γ_2 Subunit—The electrophysiological analysis in this study brought out two major points about the modulation of neuronal Ca^{2+} channels by the γ_2 subunit. First, the main function of the γ_2 subunit on neuronal Ca^{2+} channels seems to be an inhibitory effect on functional activity of these channels. There were strong and consistent inhibitory effects of γ_2 on current amplitude (37–40%) through all of our experiments (Figs. 2 and 5). The activation kinetics of the α_{1B}-class Ca^{2+} channel was also significantly decelerated by γ_2 co-expression (Fig. 4, *C* and *D*). Consistent with our finding, the patch clamp studies of the stargazer mouse showed 40% decrease of current amplitude of high voltage-activated Ca^{2+} channels (30). Moreover, recent studies of γ_1 null mice reported an increase of current amplitude of Ca^{2+} channel as the main alteration after γ_1 gene ablation in skeletal muscle (33, 34). In addition, the consistent γ_2 inhibitory effect *in vitro* and *in vivo* suggests that the down-regulation of neuronal Ca^{2+} channel activity by the γ_2 subunit may be important for the prevention of neuronal hyperexcitability that has been suggested as a mechanism of epilepsy in the stargazer mouse.

Second, our results suggest that the inhibitory effect of γ_2 on current amplitude depends on the co-expression of the $\alpha_2\delta$ subunit. The experimental results in Figs. 2 and 4 suggest that γ_2 might counteract the $\alpha_2\delta$ effects on neuronal Ca^{2+} channels. The increase in current amplitude induced by $\alpha_2\delta$ was reversed by γ_2 co-expression (Fig. 2, *A* and *B*). The acceleration of activation kinetics by $\alpha_2\delta$ was also diminished by γ_2 co-expression (Fig. 4 (*C* and *D*) and Table I). Finally, data in Fig. 5 strongly suggest that the γ_2 subunit antagonizes the modulatory effect of $\alpha_2\delta$ on current amplitude of neuronal Ca^{2+} channels. Although the mechanism underlying the $\alpha_2\delta$-dependent inhibitory effect of the γ_2 subunit is not clear, one of the studies in the γ_1 null mice suggested that the observed Ca^{2+} channel current increase was due to the increase in channel open probability rather than an increase in the total number of channel and/or single channel conductance (33). Since the $\alpha_2\delta$ subunit is able to increase the open probability of Ca^{2+} channels (35), it is likely that the γ_2 subunit counteracts the effects of $\alpha_2\delta$ on the open probability of Ca^{2+} channels and thus the Ca^{2+} channel current amplitude. The antagonism between $\alpha_2\delta$ and γ could be involved in the fine-tuning of Ca^{2+} channel functional activity. In addition, the $\alpha_2\delta$ dependence of the γ_2 inhibitory effect could eliminate the possibility of nonspecific inhibition of γ_2 on the expression of neuronal Ca^{2+} channels in our experiments. The recombinant Ca^{2+} channels without $\alpha_2\delta$ did not show significant decrease of current amplitude by co-expression of the γ_2 subunit (Fig. 5).

Previously, Letts *et al.* (3) and Klugbauer *et al.* (10) reported that γ_2 co-expression shifted the voltage dependence of steady-state inactivation to more negative potentials but had no effect on the current amplitude of $\alpha_{1A}\beta\alpha_2\delta$ Ca^{2+} channels expressed in baby hamster kidney and HEK293 cells, respectively. It is not clear why there is this difference of the γ_2 effects on Ca^{2+} channels between the previous studies and this report. However, these inconsistencies could be associated to differences in the combination of subunits employed, the expression level of endogenous and exogenous Ca^{2+} channel subunits, the experimental setup for electrophysiological recording, and/or particular physiological conditions such as the phosphorylation status of the channels.

The Modulation of Ca^{2+} Channels by the γ_1 Subunit—Interestingly, the γ_1 subunit exerted a modulatory effect similar to that of γ_2 on neuronal Ca^{2+} channels despite its muscle-specific expression and significant primary sequence divergence between the two isoforms. The γ_1 subunit decreased current amplitude of both neuronal α_{1B}-class (Fig. 2, *A* and *B*) and α_{1A}-class channels (data not shown), and modulated the activation kinetics of α_{1B}-class channels (Fig. 4 (*C* and *D*) and Table I). Similarly, co-expression of γ_1 significantly decreased the current amplitude of $\alpha_{1C}\beta_1\alpha_2\delta$ channels in *Xenopus* oocytes (5). Likewise, as mentioned above, recent electrophysiological studies showed that the current amplitude of skeletal muscle Ca^{2+} channel (α_{1S}-class) is significantly increased in the γ_1 null mice (33, 34). Taken together, these results suggest that the γ_1 subunit could exert inhibitory effect not only on α_{1S}- but also on other Ca^{2+} channels including those of the α_{1A}-, α_{1B}-, and α_{1C}-class. However, there have been controversial reports regarding the γ_1 function. Depending on the subunit composition, γ_1 co-expression increased or decreased the current amplitude of α_{1C}- or α_{1A}-class channels expressed in oocytes or HEK 293 cells (4–6, 9). The changes in steady-state activation by γ_1 co-expression also varied in α_{1C}-class channels (5, 6, 9). The γ_1 co-expression caused a negative shift of steady-state inactivation curves of α_{1C}-class channels in some studies (5, 7, 9).

In summary, our study demonstrates the association of the γ_2 subunit with the neuronal Ca^{2+} channel complex *in vivo* and indicates an inhibitory function for the γ_2 subunit.

Acknowledgments—We thank Drs. T. P. Snutch and D. Lipscombe for providing the cDNA clones. We are also grateful to Dr. Y. M. Kobayashi and Jyothi Arikkath for helpful comments on the manuscript.

REFERENCES

1. Catterall, W. A. (1995) *Annu. Rev. Biochem.* **64,** 493–531
2. De Waard, M., Gurnett, C. A., and Campbell, K. P. (1996) in *Structural and Functional Diversity of Voltage-activated Calcium Channels* (Narahashi, T., ed) Vol. 4., pp. 41–87, Plenum Press, New York
3. Letts, V. A., Felix, R., Biddlecome, G. H., Arikkath, J., Mahaffey, C. L., Valenzuela, A., Bartlett, F. S., II, Mori, Y., Campbell, K. P., and Frankel, W. N. (1998) *Nat. Genet.* **19,** 340–347
4. Mori, Y., Friedrich, T., Kim, M.-S., Mikami, A., Nakai, J., Ruth, P., Bosse, E., Hofmann, F., Flockerzi, V., Furuichi, T., Mikoshiba, K., Imoto, K., Tanabe, T., and Numa, S. (1991) *Nature* **350,** 398–402
5. Singer, D., Biel, M., Lotan, I., Flockerzi, V., Hofmann, F., and Dascal, N. (1991) *Science* **253,** 1553–1557
6. Wei, X., Perez-Reyes, E., Lacerda, A. E., Schuster, G., Brown, A. M., and Birnbaumer, L. (1991) *J. Biol. Chem.* **266,** 21943–21947
7. Lerche, H., Klugbauer, N., Lehmann-Horn, F., Hofmann, F., and Melzer, W. (1996) *Pflugers Arch.* **431,** 461–463
8. Suh-Kim, H., Wei, X., and Birnbaumer, L. (1996) *Mol. Pharmacol.* **50,** 1330–1337
9. Eberst, R., Dai, S., Klugbauer, N., and Hofmann, F. (1997) *Pflugers Arch.* **433,** 633–637
10. Klugbauer, N., Dai, S., Specht, V., Lacinova, L., Marais, E., Bohn, G., and Hofmann, F. (2000) *FEBS Lett.* **470,** 189–197
11. Burgess, D. L., Davis, C. F., Gefrides, L. A., and Noebels, J. L. (1999) *Genome Res.* **9,** 1204–1213
12. Chen, L., Chetkovich, D. M., Petralia, R. S., Sweeney, N. T., Kawasaki, Y., Wenthold, R. J., Bredt, D. S., and Nicoll, R. A. (2000) *Nature* **408,** 936–943
13. Fletcher, C. F., Lutz, C. M., O'Sullivan, T. N., Shaughnessy, J. D., Jr., Hawkes,

R., Frankel, W. N., Copeland, N. G., and Jenkins, N. A. (1996) *Cell* **87,** 607–617
14. Mori, Y., Wakamori, M., Oda, S., Fletcher, C. F., Sekiguchi, N., Mori, E., Copeland, N. G., Jenkins, N. A., Matsushita, K., Matsuyama, Z., and Imoto, K. (2000) *J. Neurosci.* **20,** 5654–5662
15. Zwingman, T. A., Neumann, P. E., Noebels, J. L., and Herrup, K. (2001) *J. Neurosci.* **21,** 1169–1178
16. Burgess, D. L., Jones, J. M., Meisler, M. H., and Noebels, J. L. (1997) *Cell* **88,** 385–392
17. Balaguero, N., Barclay, J., Mione, M., Canti, C., Brodbeck, J., Gardiner, R. M., Rees, M., and Dolphin, A. C. (2000) *Society for Neuroscience 30th Annual Meeting New Orleans, November 4–9, 2000,* Abstract 135 9, p. 365, Society for Neuroscience, Washington, D. C.
18. Witcher, D. R., De Waard, M., Kahl, S. D., and Campbell, K. P. (1994) *Methods Enzymol.* **238,** 335–348
19. Witcher, D. R., De Waard, M., and Campbell, K. P. (1993) *Neuropharmacology* **32,** 1127–1139
20. Liu, J., De Waard, M., Scott, V. E. S., Gurnett, C. A., Lennon, V. A., and Campbell, K. P. (1996) *J. Biol. Chem.* **271,** 13804–13810
21. Gurnett, C. A., and Campbell, K. P. (1996) *J. Biol. Chem.* **271,** 27975–27978
22. Witcher, D. R., De Waard, M., Sakamoto, J., Franzini-Armstrong, C., Pragnell, M., Kahl, S. D., and Campbell, K. P. (1993) *Science* **261,** 486–489
23. Sakamoto, J., and Campbell, K. P. (1991) *J. Biol. Chem.* **266,** 18914–18919
24. Harlow, E., and Lane, D. (1999) *Using Antibodies: A Laboratory Manual,* Cold Spring Harbor Laboratory Press, Cold Spring Harbor, NY
25. Lin, Z., Haus, S., Edgerton, J., and Lipscombe, D. (1997) *Neuron* **18,** 153–166
26. Jay, S. D., Ellis, S. B., McCue, A. F., Williams, M. E., Vedvick, T. S., Harpold, M. M., and Campbell, K. P. (1990) *Science* **248,** 490–492
27. Goldin, A. L., and Sumikawa, K. (1992) *Methods Enzymol.* **207,** 279–297
28. Stuhmer, W. (1992) *Methods Enzymol.* **207,** 319–339
29. Wakamori, M., Mikala, G., and Mori, Y. (1999) *J. Physiol.* (*Lond.*) **517,** 659–672
30. Zhang, Y., and Noebels, J. L. (2000) *Society for Neuroscience 30th Annual Meeting New Orleans, November 4–9, 2000*, Abstract 135 3, p. 364, Society for Neuroscience, Washington, D. C.
31. Black, J. L., III, and Lennon, V. A. (1999) *Mayo Clin. Proc.* **74,** 357–361
32. Burgess, D. L., Biddlecome, G. H., McDonough, S. I., Diaz, M. E., Zilinski, C. A., Bean, B. P., Campbell, K. P., and Noebels, J. L. (1999) *Mol. Cell. Neurosci.* **13,** 293–311
33. Freise, D., Held, B., Wissenbach, U., Pfeifer, A., Trost, C., Himmerkus, N., Schweig, U., Freichel, M., Biel, M., Hofmann, F., Hoth, M., and Flockerzi, V. (2000) *J. Biol. Chem.* **275,** 14476–144781
34. Ahern, C., Powers, P., Biddlecomb, G., Roethe, L., Vallejo, P., Mortenson, L., Strube, C., Campbell, K., Coronado, R., Gregg, R. (2001) *BMC Physiol.* **1,** 8
35. Shistik, E., Ivanina, T., Puri, T., Hosey, M., and Dascal, N. (1995) *J. Physiol.* (*Lond.*) **489,** 55–62